Supplementary for
A Closer Look at the Robustness of Contrastive Language-Image Pre-Training (CLIP)

In Section A, we introduce the experimental details including the training details, datasets and computation resources. Then, we report the full results of factor-level robustness in Section B; In Section C, we compare the OOD detection performance of zero-shot CLIP using maximum concept matching [1] and other models using maximum logit [2]; Lastly, we show the calibration performance of models on ImageNet-Rendition [3], ObjectNet [4] and ImageNet-Vid-Robust [5] (Section D).

A Experimental Setup

A.1 Datasets

We carefully check the licenses of all datasets and list the open sources to them.

Datasets used in factor-level robustness:

`ImageNet` [6] (https://www.image-net.org);
`ImageNet-X` [7] (https://github.com/facebookresearch/imagenetx);

Factor	Number of samples
Pose	16080
Background	15441
Pattern	6571
Color	6476
Smaller	1473
Shape	696
Partial View	678
Subcategory	614
Texture	286
Larger	157
Darker	125
Object Blocking	78
Person Blocking	61
Style	45
Brighter	45
Multiple Objects	40
Overall	48868

Table A-1: **Statistics of ImageNet-X of each factor.**

Datasets used in out-of-distribution detection:

`iNaturalist` [8] (https://www.kaggle.com/c/inaturalist-2021);
`SUN` [9] (https://groups.csail.mit.edu/vision/SUN/hierarchy.html);

37th Conference on Neural Information Processing Systems (NeurIPS 2023).

TEXTURE [10] (https://www.robots.ox.ac.uk/ vgg/data/dtd/);
PLACES [11] (https://github.com/CSAILVision/places365);
ImageNet-O [9] (https://github.com/hendrycks/natural-adv-examples);

Datasets used in predictive uncertainty:

ImageNet-V2 [5] (https://github.com/modestyachts/ImageNetV2);
ImageNet-Adversarial [9] (https://github.com/hendrycks/natural-adv-examples);
ImageNet-Rendition [3] (https://github.com/hendrycks/robustness);
ImageNet-Sketch [12] (https://github.com/HaohanWang/ImageNet-Sketch);
ObjectNet [4] (https://objectnet.dev/download.html);
ImageNet-Vid-Robust [5] (https://github.com/modestyachts/imagenet-vid-robust-example).

A.2 Models Included in Experiments

A.2.1 Zero-shot CLIP

We use the zero-shot CLIP models provided in OpenCLIP [13]. They are listed as follows in the pattern (architecture, source):

(RN50, openai)

(RN50-quickgelu, openai)

(RN101, openai)

(RN101-quickgelu, openai)

(RN50×4, openai)

(RN50×16, openai)

(RN50×64, openai)

(ViT-B-32, openai)

(ViT-B-32-quickgelu, openai)

(ViT-B-16, openai)

(ViT-L-14, openai)

(ViT-L-14-336, openai)

(ViT-B-32, laion400m_e31)

(ViT-B-32, laion400m_e32)

(ViT-B-32, laion2b_e16)

(ViT-B-32, laion2b_s34b_b79k)

(ViT-B-32-quickgelu, laion400m_e31)

(ViT-B-32-quickgelu, laion400m_e32)

(ViT-B-16, laion400m_e31)

(ViT-B-16, laion400m_e32)

(ViT-B-16, laion2b_s34b_b88k)

(ViT-B-16-plus-240, laion400m_e31)

(ViT-B-16-plus-240, laion400m_e32)

(ViT-L-14, laion400m_e31)

(ViT-L-14, laion400m_e32)

(ViT-L-14, laion2b_s32b_b82k)

(ViT-H-14, laion2b_s32b_b79k)

(ViT-g-14, laion2b_s12b_b42k)

(ViT-g-14, laion2b_s34b_b88k)

(ViT-bigG-14, laion2b_s39b_b160k)

(convnext_base, laion400m_s13b_b51k)

(convnext_base_w, laion2b_s13b_b82k)

(convnext_base_w, laion2b_s13b_b82_augreg)

(convnext_base_w, laion_aesthetic_s13b_b82k)

(convnext_base_w_320, laion_aesthetic_s13b_b82k)

(convnext_base_w_320, laion_aesthetic_s13b_b82k_augreg)

(convnext_large_d, laion2b_s26b_b102k_augreg)

(convnext_large_d_320, laion2b_s29b_b131k_ft)

(convnext_large_d_320, laion2b_s29b_b131k_ft_soup)

(convnext_xxlarge, laion2b_s34b_b82k_augreg)

(convnext_xxlarge, laion2b_s34b_b82k_augreg_rewind)

(convnext_xxlarge, laion2b_s34b_b82k_augreg_soup)

Nine models provided by Cherti et al. [14]: https://github.com/LAION-AI/scaling-laws-openclip:

(ViT-B-32, Model-B-32_Data-80M_Samples-3B_lr-5e-4_bs-32k.pt)

(ViT-B-32, Model-B-32_Data-80M_Samples-13B_lr-5e-4_bs-32k.pt)

(ViT-B-32, Model-B-32_Data-80M_Samples-34B_lr-1e-3_bs-88k.pt)

(ViT-B-16, Model-B-16_Data-80M_Samples-3B_lr-1e-3_bs-88k.pt)

(ViT-B-16, Model-B-16_Data-80M_Samples-13B_lr-1e-3_bs-88k.pt)

(ViT-B-16, Model-B-16_Data-80M_Samples-34B_lr-1e-3_bs-88k.pt)

(ViT-L-14, Model-L-14_Data-80M_Samples-3B_lr-1e-3_bs-88k.pt)

(ViT-L-14, Model-L-14_Data-80M_Samples-13B_lr-1e-3_bs-88k.pt)

(ViT-L-14, Model-L-14_Data-80M_Samples-34B_lr-1e-3_bs-88k.pt)

A.2.2 Fine-tuned CLIP on ImageNet

We consider the fine-tuned CLIP models provided in TIMM [15]. They are listed as follows:

vit_huge_patch14_clip_336.laion2b_ft_in12k_in1k

vit_huge_patch14_clip_224.laion2b_ft_in12k_in1k

vit_large_patch14_clip_336.laion2b_ft_in12k_in1k

vit_large_patch14_clip_224.laion2b_ft_in12k_in1k

vit_base_patch16_clip_384.laion2b_ft_in12k_in1k

vit_base_patch16_clip_224.laion2b_ft_in12k_in1k

vit_base_patch32_clip_448.laion2b_ft_in12k_in1k

vit_base_patch32_clip_384.laion2b_ft_in12k_in1k

vit_base_patch32_clip_224.laion2b_ft_in12k_in1k

vit_huge_patch14_clip_224.laion2b_ft_in1k

vit_large_patch14_clip_336.laion2b_ft_in1k

vit_large_patch14_clip_224.laion2b_ft_in1k vit_base_patch16_clip_384.laion2b_ft_in1k

vit_base_patch16_clip_224.laion2b_ft_in1k

vit_base_patch32_clip_224.laion2b_ft_in1k

vit_large_patch14_clip_336.openai_ft_in12k_in1k

vit_large_patch14_clip_224.openai_ft_in12k_in1k

vit_base_patch16_clip_384.openai_ft_in12k_in1k

vit_base_patch16_clip_224.openai_ft_in12k_in1k

vit_base_patch32_clip_384.openai_ft_in12k_in1k

vit_large_patch14_clip_224.openai_ft_in1k

vit_base_patch16_clip_384.openai_ft_in1k

vit_base_patch16_clip_224.openai_ft_in1k

vit_base_patch32_clip_224.openai_ft_in1k

convnext_base.clip_laion2b_augreg_ft_in1k

convnext_base.clip_laiona_augreg_ft_in1k_384

convnext_large_mlp.clip_laion2b_augreg_ft_in1k

convnext_large_mlp.clip_laion2b_augreg_ft_in1k_384

convnext_large_mlp.clip_laion2b_soup_ft_in12k_in1k_384

convnext_large_mlp.clip_laion2b_soup_ft_in12k_in1k_320

convnext_base.clip_laion2b_augreg_ft_in12k_in1k_384

convnext_base.clip_laion2b_augreg_ft_in12k_in1k

A.2.3 Other ImageNet Models

The standard models and those which are pre-trained on more data are publicly available on TIMM as well. We refer to the supplementary of Taori et al. [16] and Deng et al. [17] for more details. For models trained by contrastive learning, they are provided by Geirhos et al. [18] in https://github.com/bethgelab/model-vs-human. They are:

PIRL [19]

InsDis [20]

MoCo [21]

MoCoV2 [22]

InfoMin [23]

simclr_resnet50×1, simclr_resnet50×2, simclr_resnet50×4 [24]

A.3 Computation Resources

PyTorch version is 1.10.0+cu111 and timm version is 0.8.21dev0. All experiment is run on one 3090 and the CPU AMD EPYC 7343 16-Core Processor.

B Full Results on Visual Factor-level Robustness

In the main paper, we report the results on 10 visual factors which contain over 150 test samples. Here, we additionally report the visual factor-level robustness on another 6 factors, and they have less than 150 test samples. The statistics of visual factors are summarized in Table A-1. As shown in Figure A-1, on the new 6 visual factors, we observe that CLIP models tend to have higher factor-level robustness. Moreover, by looking at CLIP models trained on WIT and LAION, we still observe that the training sources lead to different trends in CLIP models.

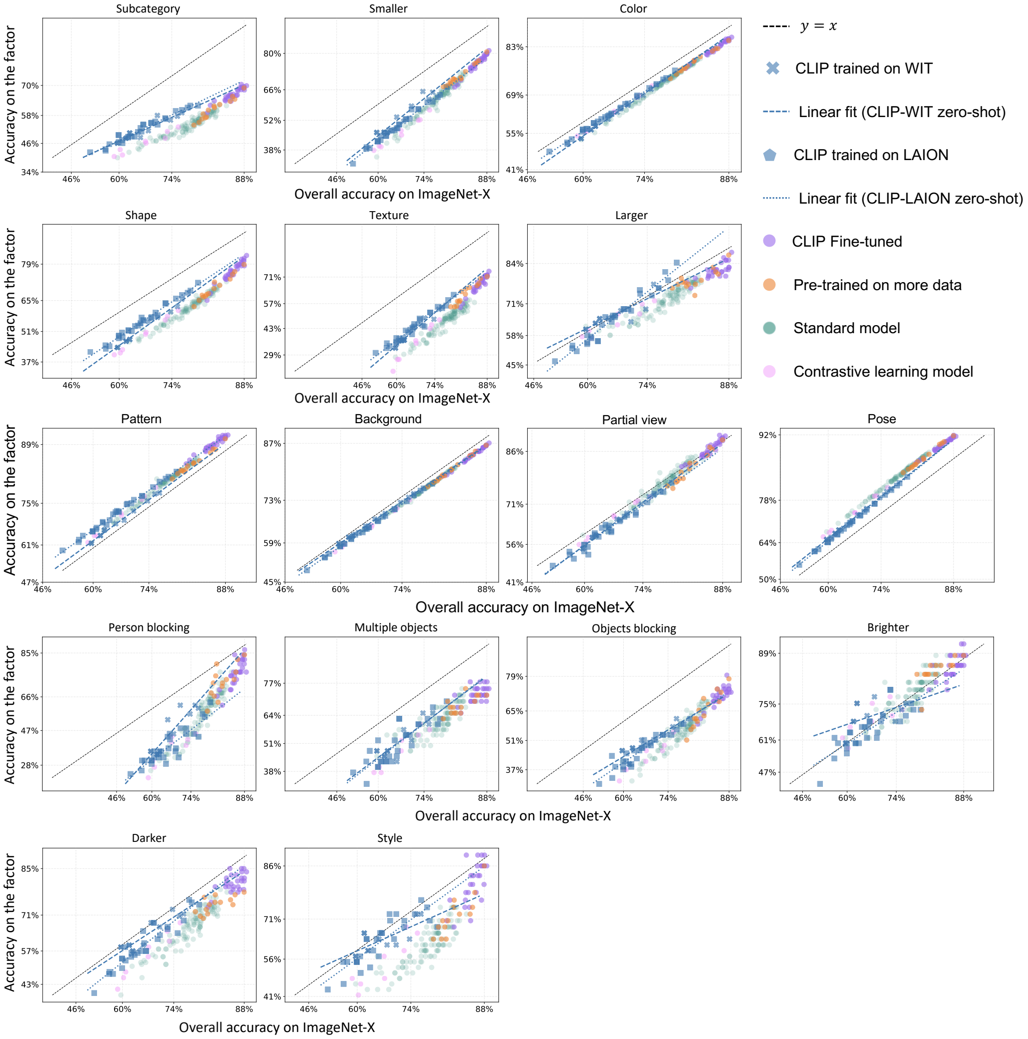

Figure A-1: **Accuracy on a factor *v.s.* overall accuracy on ImageNet-X on 16 factors.** We additionally include another 6 factors: *Person blocking*, *Multiple objects*, *Object blocking*, *Brighter*, *Darker* and *Color*, and the number of images labeled by these factors is no more than 150. We further observe that CLIP models tend to be more robust than other ImageNet models on these factors.

C More Results on Out-of-distribution Detection

In the main paper, we use the maximum softmax score as the detection method for the models that are trained or fine-tuned on ImageNet. Here, we instead use maximum logit [2] for them. Zero-shot CLIP models still use maximum concept matching [1].

As shown in Figure A-2, CLIP models remain competitive with other models. Moreover, the observations reported in the main paper (Section 5) still hold. Specifically, 1) CLIP-FT models fine-tuned on ImageNet-1K do not exhibit a clear correlation between OOD detection performance and classification accuracy. 2) With similar in-distribution accuracy, CLIP models tend to achieve competitive or higher OOD detection performance compared to other groups of models. 3) We find that additional fine-tuning on ImageNet-12K substantially improves the model's ability to detect OOD examples compared to those directly fine-tuned on ImageNet-1K.

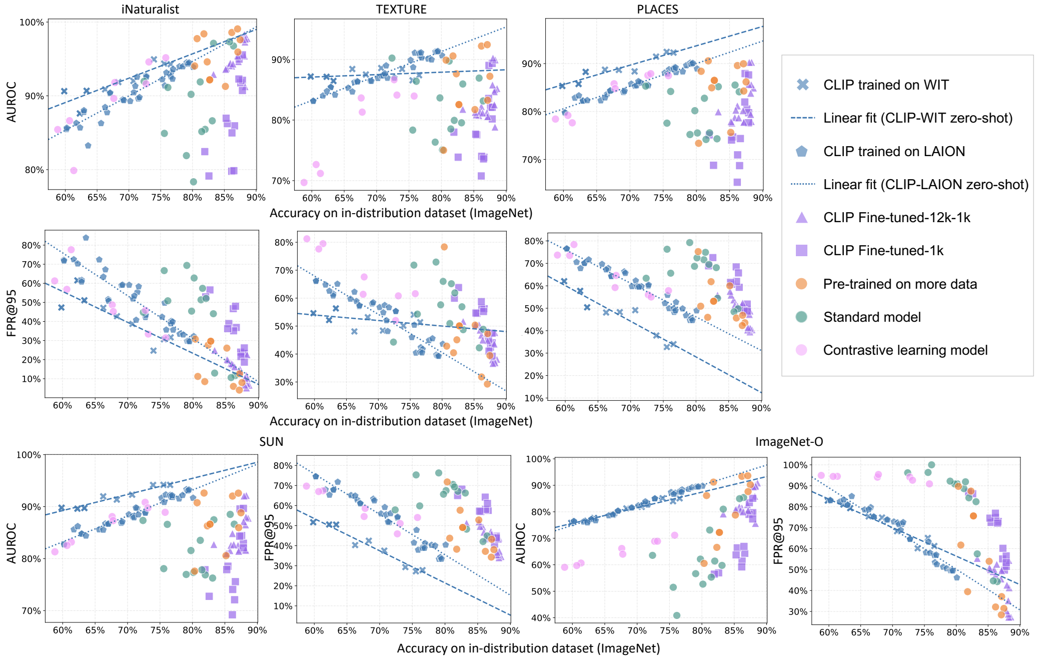

Figure A-2: **Performance of OOD detection *v.s.* accuracy on ImageNet.** The OOD detection ability is measured by AUROC (↑) and FPR@95 (↓). Each point represents a model. We plot the results on iNaturalist, SUN, PLACES, TEXTURE and ImageNet-O. The blue straight lines are fit with robust linear regression [25]. We observe that training distribution has a greater impact than training dataset quantity on the OOD detection performance of CLIP. For CLIP models from the same source, their ID accuracy correlates with OOD detection performance. Moreover, after additionally fine-tuning on ImageNet-12K, CLIP models are generally better at detecting OOD samples than those directly fine-tuned on ImageNet-1K.

Moreover, we include the results of OOD detection performance on NINCO [26] in Figure A-3. We find the observations on this dataset consistent with those on five standard OOD detection benchmarks: 1) for CLIP models from the same source, their ID accuracy correlate with OOD detection; 2) training source influences trends of CLIP; 3) fine-tuning procedure influences OOD detection ability of CLIP. We use following models:

`vit_base_patch16_384`, `vit_base_patch16_224_21kpre`,

`swinv2-1k`, `swinv2-22k`,

`deit3-384-1k`, `deit3_base_patch16_224`,

`xcit_medium_24_p16_224`, `xcit_medium_24_p16_224_dist`, `convnext_base`, `convnext_base_in22ft1k`,

`BiT_s`, `BiT_m`,

`tf_efficientnetv2_m`, `tf_efficientnetv2_m_in21ft1k`,

`resnet50`, `resnet18.tv_in1k`, `'resnet34.tv_in1k'`,

`efficientnet_b0`, `tf_efficientnet_b1.in1k`, `tf_efficientnet_b7`,

`repvgg_b0.rvgg_in1k`,

`inception_v4.tf_in1k`,

`mobilenetv2_050.lamb_in1k`,

`deit3-384-22k`, `deit3_base_patch16_224_in21ft1k`

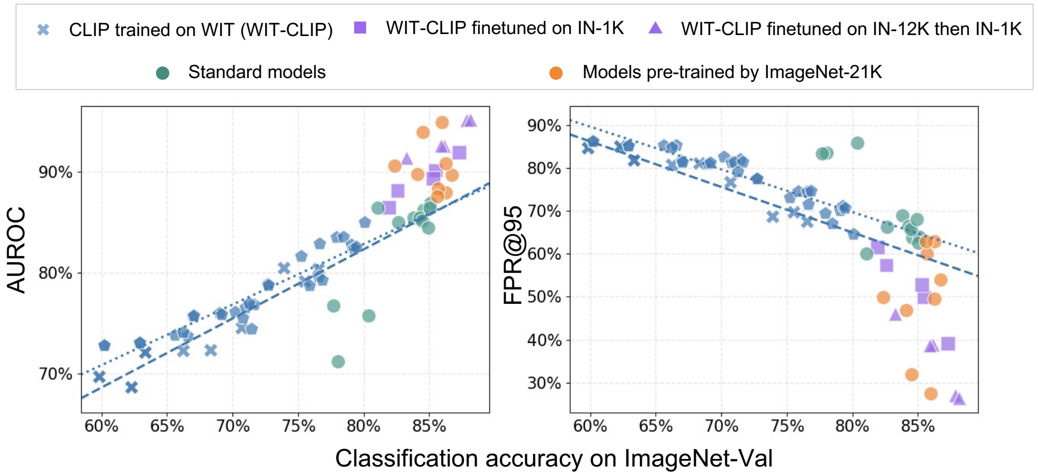

Figure A-3: **New benchmark results on NINCO for OOD detection.** Classification accuracy on ImageNetVal vs. model OOD detection measured by classes mean AUROC (↑) and classes mean FPR@95 (↓). Standard models and models pretrained on IN-21K use MSP.

D More Results on Predictive Uncertainty

We show the full results of uncertainty estimation of all models on all datasets: ImageNet-Val (ID test set), ImageNet-V2-A, ImageNet-A, ImageNet-S, ImageNet-R, ObjectNet and ImageNet-Vid-Robust in Figure A-4. We use estimated calibration error (ECE) and negative log-likelihood (NLL) as evaluation metrics. We also report the results after calibration using temperature scaling. As for the calibration, following the protocol in [27], we divide the validation set of ImageNet into two halves: one for temperature scaling (ID calibration set), and the other one for ID test.

E Experiments on MAE models

Figure A-5 shows the performance of models pre-trained by MAE[28] on factor level robustness, OOD detection and calibration. MAE is not a contrastive training approach in contrast to MoCo and SimCLRV2. We see that: 1) Visual factor-level robustness: three MAE models lie on the area of models pre-trained on more data; 2) OOD detection: MAE models also lie in the area with other models pre-trained on more data. Some zero-shot CLIP models achieve higher performance than MAE models; 3) Calibration: before TS, MAE models have higher uncertainty estimation performance than CLIP trained on LAION while lower than CLIP trained on WIT. Post TS, CLIP models become better than MAE.

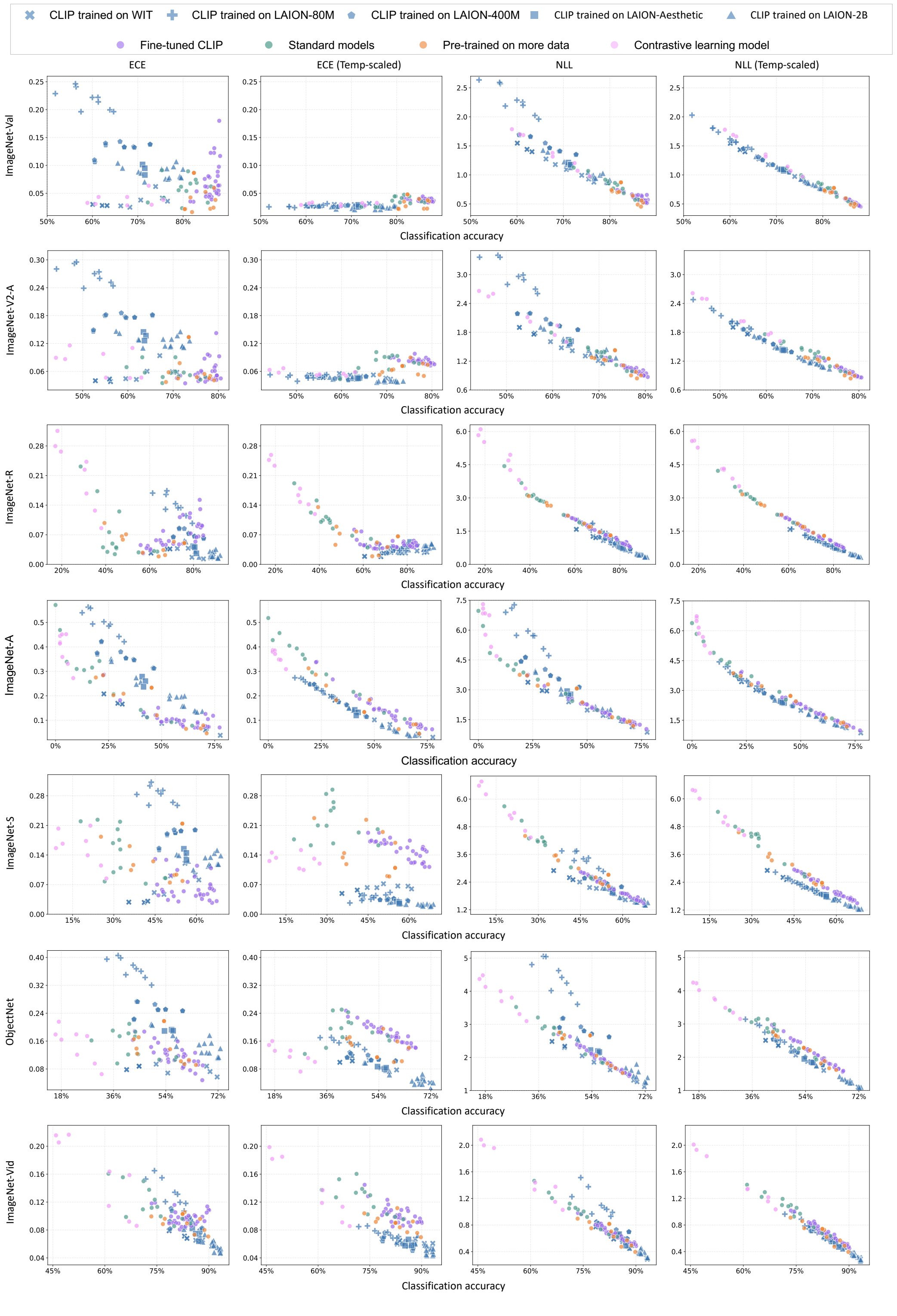

Figure A-4: **Performance of uncertainty estimation *v.s.* classification accuracy.** We report results on 7 datasets, using ECE (↓) and NLL (↓). We also include calibration performance after calibration with temperature scaling. Each point represents a model. We use colors to represent model groups. For zero-shot CLIP models, we use shapes to indicate training distribution and quantity.

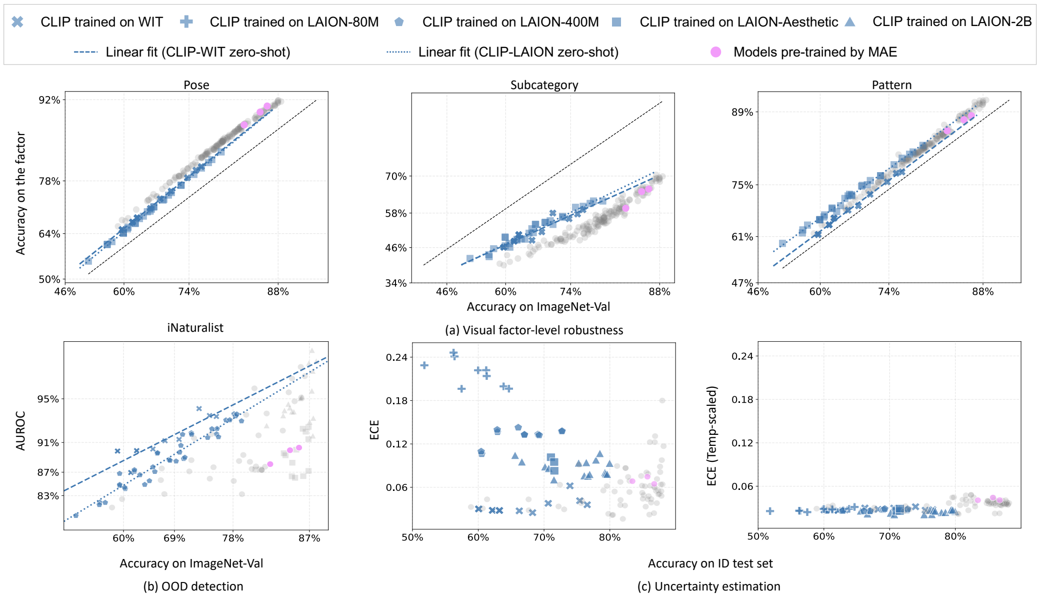

(a) Visual factor-level robustness

(b) OOD detection

(c) Uncertainty estimation

Figure A-5: We evaluate three models pre-trained by MAE. **(a)** The models performance on the subset of ImageNetX annotated with a given visual factor (y-axis) to their overall accuracy on the whole ImageNet-X (x-axis). **(b)** OOD detection capability of models vs. ID dataset classification accuracy. **(c)** Model calibration performance with respect to their classification accuracy.

F Analysis on Retrieval performance of Zero-shot CLIPs

Figure A-6 illustrates the image classification accuracy on ImageNet validation set versus their zero-shot retrieval performance of CLIP models on MS-COCO2017. We find that the zero shot retrieval performance correlate with its classification accuracy. CLIPs trained on different dataset distribution lie on different trends. Such correlation shows that the ability of image classification is predictive of their image or text retrieval capability. Interestingly, we observe there are four specific ConvNeXt-based CLIP models that significantly depart from the trend of LAION. We notice that they are trained with a limited random resize crop range (0.9, 1.0), which may hurt the capability of learned embeddings.

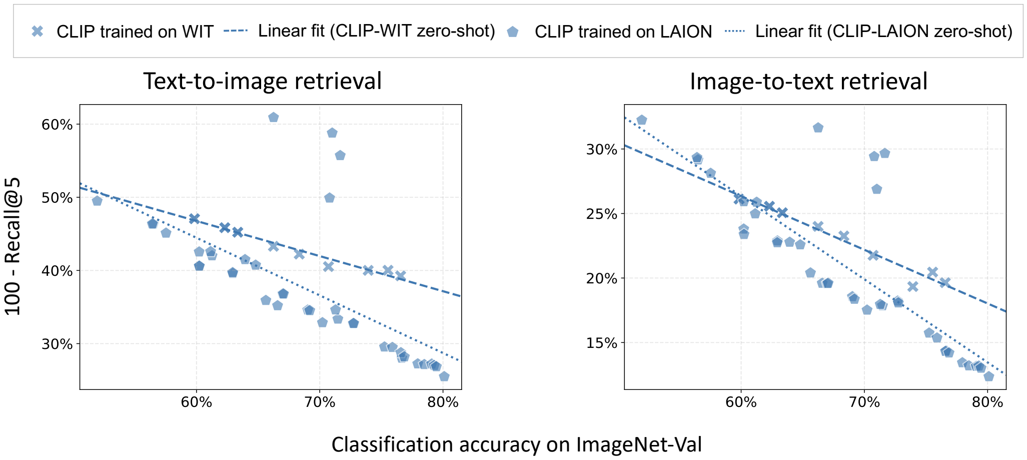

Figure A-6: Classification accuracy vs. retrieval performance measured by (100 – Recall@5) (↓).

References

[1] Yifei Ming, Ziyang Cai, Jiuxiang Gu, Yiyou Sun, Wei Li, and Yixuan Li. Delving into out-of-distribution detection with vision-language representations. In *Advances in Neural Information Processing Systems*, 2022. A-1, A-6

[2] Dan Hendrycks, Steven Basart, Mantas Mazeika, Andy Zou, Joe Kwon, Mohammadreza Mostajabi, Jacob Steinhardt, and Dawn Song. Scaling out-of-distribution detection for real-world settings. In *International Conference on Machine Learning*, 2022. A-1, A-6

[3] Dan Hendrycks, Steven Basart, Norman Mu, Saurav Kadavath, Frank Wang, Evan Dorundo, Rahul Desai, Tyler Zhu, Samyak Parajuli, Mike Guo, et al. The many faces of robustness: A critical analysis of out-of-distribution generalization. In *Proceedings of the IEEE/CVF International Conference on Computer Vision*, pages 8340–8349, 2021. A-1, A-2

[4] Andrei Barbu, David Mayo, Julian Alverio, William Luo, Christopher Wang, Dan Gutfreund, Josh Tenenbaum, and Boris Katz. Objectnet: A large-scale bias-controlled dataset for pushing the limits of object recognition models. In *Advances in Neural Information Processing Systems*, 2019. A-1, A-2

[5] Vaishaal Shankar, Achal Dave, Rebecca Roelofs, Deva Ramanan, Benjamin Recht, and Ludwig Schmidt. Do image classifiers generalize across time? In *Proceedings of the IEEE/CVF International Conference on Computer Vision*, pages 9661–9669, 2021. A-1, A-2

[6] J. Deng, W. Dong, R. Socher, L.-J. Li, K. Li, and L. Fei-Fei. ImageNet: A Large-Scale Hierarchical Image Database. In *Proceedings of the IEEE Conference on Computer Vision and Pattern Recognition*, 2009. A-1

[7] Badr Youbi Idrissi, Diane Bouchacourt, Randall Balestriero, Ivan Evtimov, Caner Hazirbas, Nicolas Ballas, Pascal Vincent, Michal Drozdzal, David Lopez-Paz, and Mark Ibrahim. Imagenet-x: Understanding model mistakes with factor of variation annotations. In *International Conference on Learning Representations*, 2022. A-1

[8] Grant Van Horn, Oisin Mac Aodha, Yang Song, Yin Cui, Chen Sun, Alex Shepard, Hartwig Adam, Pietro Perona, and Serge Belongie. The inaturalist species classification and detection dataset. In *Proceedings of the IEEE Conference on Computer Vision and Pattern Recognition*, pages 8769–8778, 2018. A-1

[9] Dan Hendrycks, Kevin Zhao, Steven Basart, Jacob Steinhardt, and Dawn Song. Natural adversarial examples. In *Proceedings of the IEEE/CVF Conference on Computer Vision and Pattern Recognition*, pages 15262–15271, 2021. A-1, A-2

[10] Mircea Cimpoi, Subhransu Maji, Iasonas Kokkinos, Sammy Mohamed, and Andrea Vedaldi. Describing textures in the wild. In *Proceedings of the IEEE Conference on Computer Vision and Pattern Recognition*, pages 3606–3613, 2014. A-2

[11] Bolei Zhou, Agata Lapedriza, Aditya Khosla, Aude Oliva, and Antonio Torralba. Places: A 10 million image database for scene recognition. *IEEE Transactions on Pattern Analysis and Machine Intelligence*, 40(6):1452–1464, 2017. A-2

[12] Haohan Wang, Songwei Ge, Zachary Lipton, and Eric P Xing. Learning robust global representations by penalizing local predictive power. In *Advances in Neural Information Processing Systems*, 2019. A-2

[13] Gabriel Ilharco, Mitchell Wortsman, Ross Wightman, Cade Gordon, Nicholas Carlini, Rohan Taori, Achal Dave, Vaishaal Shankar, Hongseok Namkoong, John Miller, Hannaneh Hajishirzi, Ali Farhadi, and Ludwig Schmidt. Openclip, July 2021. URL `https://doi.org/10.5281/zenodo.5143773`. If you use this software, please cite it as below. A-2

[14] Mehdi Cherti, Romain Beaumont, Ross Wightman, Mitchell Wortsman, Gabriel Ilharco, Cade Gordon, Christoph Schuhmann, Ludwig Schmidt, and Jenia Jitsev. Reproducible scaling laws for contrastive language-image learning. In *Proceedings of the IEEE Conference on Computer Vision and Pattern Recognition*, 2023. A-3

[15] Ross Wightman. Pytorch image models. `https://github.com/rwightman/pytorch-image-models`, 2019. A-3

[16] Rohan Taori, Achal Dave, Vaishaal Shankar, Nicholas Carlini, Benjamin Recht, and Ludwig Schmidt. Measuring robustness to natural distribution shifts in image classification. In *Advances in Neural Information Processing Systems*, pages 18583–18599, 2020. A-4

[17] Weijian Deng, Stephen Gould, and Liang Zheng. On the strong correlation between model invariance and generalization. In *Advances in Neural Information Processing Systems*, 2022. A-4

[18] Robert Geirhos, Kantharaju Narayanappa, Benjamin Mitzkus, Tizian Thieringer, Matthias Bethge, Felix A Wichmann, and Wieland Brendel. Partial success in closing the gap between human and machine vision. In *Advances in Neural Information Processing Systems 34*, 2021. A-4

[19] Ishan Misra and Laurens van der Maaten. Self-supervised learning of pretext-invariant representations. In *Proceedings of the IEEE/CVF Conference on Computer Vision and Pattern Recognition*, pages 6707–6717, 2020. A-4

[20] Zhirong Wu, Yuanjun Xiong, Stella X Yu, and Dahua Lin. Unsupervised feature learning via non-parametric instance discrimination. In *Proceedings of the IEEE Conference on Computer Vision and Pattern Recognition*, pages 3733–3742, 2018. A-4

[21] Kaiming He, Haoqi Fan, Yuxin Wu, Saining Xie, and Ross Girshick. Momentum contrast for unsupervised visual representation learning. In *Proceedings of the IEEE/CVF Conference on Computer Vision and Pattern Recognition*, pages 9729–9738, 2020. A-4

[22] Xinlei Chen, Haoqi Fan, Ross Girshick, and Kaiming He. Improved baselines with momentum contrastive learning. *arXiv preprint arXiv:2003.04297*, 2020. A-4

[23] Yonglong Tian, Chen Sun, Ben Poole, Dilip Krishnan, Cordelia Schmid, and Phillip Isola. What makes for good views for contrastive learning? In *Advances in Neural Information Processing Systems*, pages 6827–6839, 2020. A-4

[24] Ting Chen, Simon Kornblith, Mohammad Norouzi, and Geoffrey Hinton. A simple framework for contrastive learning of visual representations. In *International Conference on Machine Learning*, pages 1597–1607. PMLR, 2020. A-4

[25] Peter J Huber. Robust statistics. In *International Encyclopedia of Statistical Science*, pages 1248–1251. Springer, 2011. A-6

[26] Julian Bitterwolf, Maximilian Müller, and Matthias Hein. In or out? fixing imagenet out-of-distribution detection evaluation. 2023. A-6

[27] Kartik Gupta, Amir Rahimi, Thalaiyasingam Ajanthan, Thomas Mensink, Cristian Sminchisescu, and Richard Hartley. Calibration of neural networks using splines. In *International Conference on Learning Representations*, 2021. URL `https://openreview.net/forum?id=eQe8DEWNN2W`. A-7

[28] Kaiming He, Xinlei Chen, Saining Xie, Yanghao Li, Piotr Dollár, and Ross Girshick. Masked autoencoders are scalable vision learners. In *Proceedings of the IEEE/CVF Conference on Computer Vision and Pattern Recognition*, pages 16000–16009, 2022. A-7